The following manuscript entitled “An investigation into the effect of fine lactose particles on the fluidization behaviour and aerosolization performance of carrier-based dry powder inhaler formulations” has been published in AAPS PharmSciTech 2014 Aug;15(4):898-909.
Epub 2014 Apr 23.

doi: 10.1208/s12249-014-0119-6.

The copyedited version can be downloaded at
http://link.springer.com/article/10.1208%2Fs12249-014-0119-6

An investigation into the effect of fine lactose particles on the fluidization behaviour and aerosolization performance of carrier-based dry powder inhaler formulations

Hanne Kinnunen[1], Gerald Hebbink[2], Harry Peters[2], Jagdeep Shur[1] and Robert Price[1*]

[1]Pharmaceutical Surface Science Research Group, Department of Pharmacy and Pharmacology, University of Bath, BA2 7AY, Bath, UK

[2] DFE Pharma, Klever Strasse 187, 47574 Goch, Germany.

***Corresponding author:**

Robert Price PhD,

Telephone: +44 (0) 1225 383644; Fax: +44 (0) 1225 386114

E-mail: r.price@bath.ac.uk

Abstract

The effect of milled and micronized lactose fines on the fluidization and *in vitro* aerosolization properties of dry powder inhaler (DPI) formulations was investigated, and the suitability of static and dynamic methods for characterising general powder flow properties of these blends was assessed. Lactose carrier pre-blends were prepared by adding different lactose fines (Lactohale 300, 230 and 210) with coarse carrier lactose (Lactohale100) at 2.5, 5, 10 and 20 wt-% concentrations. Powder flow properties of lactose pre-blends were characterized using the Freeman Technology FT4 and Schulze RST-XS ring shear tester. A strong correlation was found between the basic flow energy (BFE_{Norm}) measured using the Freeman FT4 rheometer and the flowability number (ff_c) measured on Schulze RST-XS. These data indicate that both static and dynamic methods are suitable for characterising general powder flow properties of lactose carriers. Increasing concentration of fines corresponded with an increase in the normalized fluidization energy (FE_{Norm}). The inclusion of fine particles of lactose resulted in a significant ($p<0.05$) increase in fine particle delivery of budesonide, and correlated with FE_{Norm}. This trend was strongest for lactose containing up to 10 wt-% LH300. A similar trend was found for the milled lactose grades LH230 and LH210. However, the increase in FE_{Norm} upon addition of milled fines only corresponded to a very slight improvement in the performance. These data suggest that whilst the fluidization energy correlated with fine particle delivery, this relationship is specific to lactose grades of similar particle size.

Keywords: Lactose, dry powder inhaler, powder flow, fluidisation

Introduction

Dry powder inhalers (DPI) are one of the most popular systems for delivering therapeutic agents for the treatment asthma and chronic obstructive pulmonary disease (COPD) via the lung (1). In carrier-based DPIs, the active pharmaceutical ingredient (API) is delivered to the lungs from a static powder bed that is fluidized and entrained by the airflow generated by the patient's inspiratory effort (2). However, to enable the API to deposit in the lungs, the API must be micronized to achieve a particle size of less than 5 µm (3). In terms of their fluidization properties, micronized powders are classified as Geldart group C powders, which are cohesive and difficult to fluidize (4). This is mainly due to the ubiquitous van der Waals interactions, which dominate the gravitational forces acting on particles finer than 10 µm (5). The highly cohesive nature of micronized materials prevents accurate metering of the low doses required for inhaled drug products, and renders the material difficult to handle during the manufacturing process. To overcome the issues of handling and dosing, and to optimize the fluidization properties of DPI formulations, a micronized API is typically blended with a Geldart group A powder that can be easily aerated and fluidized (4). For carrier based DPI formulations, the Geldart group A granular material is a coarse sized fraction of lactose monohydrate.

It is also well known that the extrinsic addition of lactose fines (a Geldart group C powder) to the coarse lactose carrier (Geldart group A powder) significantly enhances the aerosolization performance and delivery of the API (6,7). The traditional theories proposed for this mechanism of action are the active site theory (8,9) and fine particle multiplet theory (6,7). The active site theory supports the hypothesis of the presence of high energy "hot-spots" on the surface of the coarse lactose. These "hot-spots" are preferentially occupied by the fine lactose particles allowing the API particles adhere to low energy sites from where they are readily dispersed upon inspiration (9-11). In contrast, the fine particle multiplet theory suggests that the improvement in DPI performance is due to the formation of mixed API/fines agglomerates that are better elutriated from the carrier particle surface than free API particles due to greater aerodynamic drag forces acting on the agglomerates (2,6,7). More recently, Shur *et al.,* reported a third possible mechanism, which suggested that the addition of lactose fines increases the cohesive strength of the formulation that in turn leads to greater deagglomeration efficiencies and an increase in fine particle delivery (12). They suggested that the increased cohesive strength of the powder bed on the addition of fine lactose particles shifted the minimum fluidization velocity of the powder bed as result of increased inter-particulate forces in the bulk powder bed. Upon reaching the minimum fluidization velocity, the cohesive powder bed fractures and the powder is fluidized as

agglomerates, which undergo increased number of high-energy particle-particle and particle-device collisions. The increased energy from these collisions enhances API re-suspension (12). Whilst studies by Versteeg *et al.,* and Tuley *et al*., have shown similar observations (13,14), Shur *et al*., related the different fluidization mechanisms for powder beds with high and low fines content to powder flow measurements performed using powder rheology (12). These findings suggest the specific relevance of the Geldart classification in defining the mechanism by which the addition of relatively small concentrations of lactose fines (Geldart group C powders) can directly affect the fluidization properties of an aeratable coarse lactose (Geldart group A powder).

Therefore, as the flowability and fluidization behaviour may be particularly important in DPIs, the quantification of powder cohesion is considered to be advantageous. Powder rheology is a key approach to assess these properties and has the potential to provide valuable insight into the deagglomeration behaviour of DPIs. There are various commercially available instruments for measuring powder flow and fluidization properties, and powder rheology measurements can be divided into two different categories on the basis of the compaction state during the measurements (15); if the powder is compacted, the measurements are considered as static, and if the particles are able to move freely during the measurements the method is dynamic. For example, a Schulze ring shear tester falls into the static category, whereas the Freeman FT4 powder rheometer can be operated in both static and dynamic modes.

The Schulze ring shear tester characterizes the powder flow properties in terms of flowability number ff_c based on the incipient flow of the powder under pre-defined consolidation and shear stresses applied on the powder using theoretically well understood Mohr stress circles; for a comprehensive explanation of Mohr circles the reader is referred to (16). However, a brief description of the process of defining the ff_c using the Mohr circles is provided in the following. To define the Mohr circles for a powder, a yield locus has to be constructed. This is done by shearing a powder sample until failure under several pre-defined consolidation stresses (σ) and by plotting the consolidation stresses against the shear stresses (τ) at which the failure occurred. Based on the yield locus, two different Mohr stress circles for a powder under a certain stress can be constructed (16). One of the circles is constructed by using the end point of the yield locus, i.e. the pre-shear point (τ_{Pre}, σ_{Pre}), as intersect for the tangent between the yield locus and the larger Mohr circle. The larger Mohr circle defines the vertical consolidation stress (σ_1) of the powder at the pre-sheared state, i.e. at steady flow. The smaller Mohr stress circle intersects the origin of the graph and is tangential to the yield locus. This stress circle represents the stresses in the powder if stored

in a container without walls and is defined as the unconfined yield strength (σ_c). The flow function of a powder (ff_c) is defined as the ratio between the consolidation stress σ_1 and the unconfined yield strength σ_c as per Equation 1, and the larger the value of ff_c for a powder, the better the flow properties it exhibits (16).

$$ff_c = \frac{\sigma_1}{\sigma_c}$$ **EQUATION 1**

In contrast, the FT4 Universal Powder Rheometer methodologies are generally based on an empirical approach. In the dynamic mode, the flow properties are measured by the energy (torque) required to rotate a helical blade at a set speed while simultaneously traversing the blade in or out of a powder bed (17). This energy is called the flow energy and is the product of all the forces acting on the rheometer blade during displacement of a powder sample (17). Changes in the flow energy of a powder can also be investigated upon aeration using a controlled, dry air supply fed through a porous stainless steel disc at the base of the testing vessel containing the powder. The air throughput is adjustable to allow various levels of air velocity to be established whilst the test is in progress. As the powder reaches its minimum fluidization velocity the flow energy decreases to a minimum and plateaus. This residual flow energy is the resistance that must be overcome to fluidize a material, and is described as the fluidization energy (18, 19, 20).

Previous studies have indicated a correlation between the flow and fluidization properties of the carrier and the final DPI formulation performance (12,20-22). However, these studies were based on relatively small datasets and the carriers used have mainly been different coarse fractions of lactose. It has also been shown that the particle size distribution of the added fine lactose is an important factor in determining whether the DPI formulation performance increases as more lactose fines are added, with finer sub-cuts of the lactose known to be more effective in improving DPI performance (11, 23-25). Following on from the hypothesis of Shur *et al.* that increased cohesion of the carrier results to an increased DPI formulation performance (12), the study reported here aimed to investigate the influence of the addition of extrinsic lactose fines with different process histories (micronized vs. milled), and thus size distributions, to the bulk flow and fluidization properties of a wide range of different carriers, and aimed to investigate whether the increased cohesion would universally account for the improved DPI performance for a wide selection of lactose carriers. Furthermore, there appears to be no scientific literature comparing the results obtained by the different powder rheology systems available on the market, and therefore this study was

also to investigate the correlation between the results obtained with the two different instruments specifically for a range of lactose pre-blends.

Materials and methods

Materials

The different inhalation grades of lactose used in the study were Lactohale (LH) products (DFE Pharma, Goch, Germany) and were: a sieved grade coarse carrier LH100, micronized lactose fines LH300 and two different grades of milled lactose fines, LH230 and LH210. Micronized budesonide (Sterling S.r.l, Perugia, Italy) was used as received. The cohesive-adhesive balance (CAB) value for the sourced micronized budesonide was determined as 0.62 following a method described elsewhere (26), implying that the drug preferentially adhered to the lactose, with the interaction being 38% greater than the drug-drug interaction. Methanol and acetonitrile were of HPLC grade (Fisher Scientific, Loughborough, UK) and water was reverse osmosis purified. (Millipore, France).

Methods

Preparation of lactose pre-blends

A series of lactose pre-blends were prepared (LH300 in LH100, LH230 in LH100 and LH210 in LH100) at fines concentrations of 2.5, 5, 10 and 20 wt-% in quantities of 100 g by sandwiching each of the fines between LH100 in three layers in an earthed 500 cm^3 stainless steel vessel and blended using a Turbula T2F mixer (Glen Creston Ltd., Middlesex, UK) at 46 rpm for 60 minutes. The pre-blends were stored at 20 ± 2°C and 44% relative humidity (RH) for at least 24 hours before any further work or characterization was performed.

Particle sizing of the raw materials and the pre-blends

The particle size distributions of the lactose raw materials and the pre-blends were measured dispersed dry at a pressure of 2 bar using a Sympatec Helos laser diffraction system with an R4 lens in conjunction with a Rodos T4 disperser and a Vibri feeder, controlled by WINDOX software (all from Sympatec Gmbh, Germany). The feed rate was adjusted such that an optical concentration between 0.5 and 5% was obtained. Five repeat

measurements were taken for each of the samples and the high resolution Fraunhofer model (HRLD) was applied for calculating the particle size distribution from the scattering data.

Scanning electron microscopy

The scanning electron microscopy (SEM) for the raw materials was performed on a JEOL JSM-6480LV SEM (JEOL, Tokyo, Japan). The samples were mounted on stainless steel sample holders using sticky carbon tabs and coated with an Edwards sputter coater S150B (BOC Edwards, UK) for 5.5 minutes prior to the analysis. An acceleration voltage of 10 kV was applied for imaging.

Powder flow properties on the Schulze RST-XS

The following procedure was followed for characterizing the samples on the RST-XS annular ring shear tester controlled by RST-Control 95 software (both from Dietmar Schulze, Germany). For each test, a 30 ml annular shear cell was filled with the powder under investigation without applying force to the upper surface of the powder bed. The powder was pre-sheared with a normal stress of 1000 Pa (τ_{pre}) until steady-state flow was achieved. A yield locus was then constructed by measuring the shear stress required to cause the powder to fail under three normal stresses lower than τ_{pre} (250 Pa, 500 Pa and 750 Pa). Each powder was tested three times and the mean flowability ratio (ff_c) at 1000 Pa pre-shear stress was calculated following Equation 1. ff_c is a dimensionless parameter, which increases as powder flowability improves (27). Hence, the more cohesive the powder, the lower the value of ff_c.

Powder flow and fluidization properties on the FT4

The flow and fluidization behaviour of the lactose pre-blends were also characterized using the FT4 Powder Rheometer (Freeman Technology, Tewkesbury, UK). The FT4 is a universal powder tester with a number of different measurement programs which can be run depending on the powder properties that are of interest. All the standard measurement programs, however, require a conditioning cycle or cycles of the powder prior to any measurement. Conditioning provides a gentle displacement of the powder removing the packing history of the powder and any operator differences, and thus generates a homogenized and uniform packing of the powder at low consolidation. During measurements, the torque and the force required to keep the impeller blade moving through the powder bed at a pre-programmed speed are measured as a function of the blade height

within the powder bed. From these raw data, the flow energy of the powder can be calculated. In practice, a 25 mm bore diameter, 20 ml split vessel is filled with the powder under investigation before a conditioning cycle is run using a 23.5 mm blade that is moved downwards in a clockwise helical path with an angle of 5 degrees at 60 mm/s. The split vessel is then opened to achieve a constant powder mass in the vessel before a specific measurement program is run. During a measurement the blade is moved through the powder in an anti-clockwise motion at a tip speed of 100 mm/s and a helical angle of 5 degrees unless otherwise stated. The normalized basic flow energy (BFE_{Norm}) is the energy required to move the blade through a gram of powder. Flow rate index (FRI) is a dimensionless parameter that is the ratio between the flow energy of the powder at anti-clockwise blade motions of 10 mm/s and 100 mm/s and normalized fluidization energy (FE_{Norm}) is the energy required to move the blade through a gram of powder in an anti-clockwise motion at 100 mm/s tip speed at the minimum fluidization velocity of each of the powders.

Preparation of carrier-based DPI formulations with budesonide

The lactose pre-blends were formulated with budesonide at 0.8 wt-% concentration to produce an array of model DPI formulations for *in vitro* testing. The formulations were prepared in quantities of 40 g by using the same stainless steel vessel as for preparing the lactose pre-blends. The lactose pre-blends were sieved with an 850 µm aperture sieve to break any large agglomerates present in the pre-blends prior to formulation processing. The drug (0.32 g) was weighed and sandwiched between half of the mass of the lactose pre-blend and blended in a Turbula at 46 rpm for 10 minutes. The remaining mass of lactose was then added and blending was continued for a further 45 minutes. The formulations were sieved with a 250 µm aperture sieve to break any large agglomerates that may have formed and the formulations stored at 20 ± 2°C and 44% RH for at least 24 hours before any testing or capsule filling. The drug content uniformity of the blends was measured by taking ten random samples of 12.5 mg and determining the amount of drug in the samples by high performance liquid chromatography (HPLC).

Drug content assay by HPLC

The drug content was determined using a validated high performance liquid chromatography (HPLC) method (26), which utilized a 250 mm ODS C18 5 µm Hypersil column with an internal diameter of 4.6 mm (Thermo, Fisher Scientific, Loughborough, UK) with the oven (Jasco CO-965, Jasco, Japan) temperature set to 40°C. The mobile phase, which consisted

of 45% methanol, 35% acetonitrile and 20% water, was pumped through the system at a flow rate of 1.5 ml/min (Jasco PU-980, Jasco, Japan). 200 µl aliquots of the drug dissolved in the mobile phase were injected with the autosampler (Jasco AS-950, Jasco, Japan). Ultraviolet (UV) detection (Jasco UV-975, Jasco, Japan) at a wavelength of 244 nm was used for quantifying the amount of budesonide, which had a retention time of 3.75 minutes.

In vitro testing of the formulations

The *in vitro* performance of the formulations was tested using a Next Generation Impactor (NGI) equipped with a pre-separator (Copley Scientific, Nottingham, UK). Prior to testing, the pre-separator was filled with 15 ml of mobile phase. The NGI cups were coated with 1 %v/v silicone oil in hexane to eliminate particle bounce. Hand-filled size 3 hydroxypropylmethylcellulose (HPMC) capsules, containing 12.5 mg of the formulation each, were aerosolized into the NGI using a Rotahaler (GlaxoSmithKline, UK) and Handihaler (Boehringer Ingelheim, Germany) DPI devices. The flow rate was adjusted using the TPK critical flow control unit (Copley Scientific, Nottingham, UK) to 90 L/min for the Rotahaler and to 52 L/min for the Handihaler, which is the upper achievable flow rate through the Handihaler device (28). The duration of aerosolization was adjusted for a time representative of an inhaled volume of 4 L. Following aerosolization of two capsules, the NGI apparatus was dismantled and each part of the NGI washed down into known volumes with the HPLC mobile phase. The mass of drug deposited on each stage of the NGI, mouthpiece and inlet throat, pre-separator and the device was determined by HPLC. This protocol was repeated in triplicate for each formulation. To compare the performance of the formulations on Rotahaler and Handihaler, results were normalized by obtaining the mean mass aerodynamic diameters (MMAD) and the fine particle fraction of particles less than 5 µm calculated by extrapolation (28). The fine particle fraction was normalized to the emitted dose (FPF_{ED}).

Analysis of statistical significance

Statistical analysis of the results was performed using Minitab v15 software (Minitab Inc., Pennsylvania, USA). Comparisons were performed using one-way analysis of variance (ANOVA) with Fisher comparison confidence level set to 95% or 99% depending on the outputs evaluated.

Results and discussion

Particle size distributions and morphology of the raw materials

Representative SEM photomicrographs of the coarse lactose carrier and lactose fines are shown in Fig. 1. The coarse lactose carrier LH100 (Fig. 1A) exhibited a typical tomahawk morphology of lactose monohydrate, with intrinsic fine lactose particles adhered to the surface. Particles of micronized lactose (LH300) were below 20 µm and had irregular morphology (Fig. 1B). The micrographs of milled fines of LH230 and LH210 are shown in Fig. 1C and Fig. 1D, respectively. Both grades of milled fines were composed of particles with wider particle size distributions. In both these milled materials, only a small proportion of the particles were less than 5 µm. The coarser particles made up the bulk of the milled lactose materials and it is worth noting that the very fine lactose particles were adhering to the surfaces of these larger particles. The size and morphology of these particles was consistent with the proprietary milling process by which they are manufactured. However, the milling process is not as intense as air-jet micronization that is used for production of the micronized fines and therefore there was less generation of fine lactose particles.

The particle size distributions of the coarse (LH100) and the lactose fines, as measured by laser diffraction, are summarized in Table I. Coarse carrier lactose (LH100) had a d_{50} of 101.6 µm, whilst micronized lactose (LH300) had a median particle size of 2.41 µm, with 90% of the particles finer than 7.76 µm. Of the two milled fines used in the study, LH230 particles exhibited the smaller particle size distribution, with a d_{50} of 8.05 µm compared to a d_{50} of 14.30 µm for LH210 grade. These particle sizes are in agreement with the specifications of these commercial products (d_{50} of LH300 < 5 µm, LH230 < 10 µm and LH210 < 20 µm).

Particle size distributions of the lactose pre-blends

The proportion of fine lactose particles in the carrier has been reported in many studies to affect the performance of DPI formulations (24,25,29). The particle size distributions and the proportion of particles finer than 4.5 µm and 30 µm of the different lactose pre-blends are summarized in Table II. The proportion of intrinsic lactose fines less than 4.5 µm associated with the batch of LH100 was 1.3%. Upon the initial addition of 2.5 wt-% of micronized (LH300) fines to the coarse carrier (LH100), the proportion of particles <4.5 µm increased to 4.9%. Upon increasing the concentration of the micronized component (LH300) to 5, 10 and 20 wt-%, the cumulative percentage of fines below 4.5 µm present in the carrier blends

increased to approximately 9, 17 and 23%, respectively (Table II). Table II also shows that the addition of the LH230 fines at 2.5, 5 and 10 wt-% concentrations resulted in 2.8, 4.3 and 7.2% proportion of particles below 4.5 µm, respectively. A concentration of 20 wt-% was required to initiate a more pronounced contribution towards the fine end of the particle size distribution, whereby the percentage of particles <4.5 µm increased to approximately 12.5%. The addition of the LH210 fines had a very small contribution on the fines content of the carrier. Even upon the addition of 20 wt-%, the proportion of fine lactose particles <4.5 µm was only 6%. These data are as expected based on the fine particle content of the different grades of fine lactose used for preparing the pre-blends.

Powder flow and fluidization properties of the lactose carriers

The powder flow properties of the lactose pre-blends in terms of flowability number ff_c measured on the Schulze RST-XS are summarized in Table III. Powder cohesion can be classified according to the ff_c number; powders with ff_c values between 2 and 4 are classified as cohesive and powders with values from 4 to 10 as free flowing (16). The data in Table III indicate that, of the lactose pre-blends used in this study, the 5, 10 and 20 wt-% blends of both the micronized LH300 and milled LH230 fines were classified as cohesive according to their ff_c numbers. In the case of LH210, an addition of at least 10 wt-% of the fines was required for the pre-blends to be classified as cohesive.

The corresponding values of the normalized basic flow energy (BFE_{Norm}) of the lactose carriers using the FT4 are summarized in Table III. When comparing the values of BFE_{Norm} to the ff_c values, it was found that a BFE_{Norm} less than 20 mJ/g is associated with the formation of cohesive lactose pre-blends. The values of flow rate index (FRI) for the lactose pre-blends used in the current study are also summarized in Table III. The addition of 20 wt-% LH300 to LH100 increased the FRI to 2.41 compared to 1.02 for the LH100. The corresponding values for 20 wt-% LH230 and LH210 blends are 1.81 and 1.41, respectively. These data suggest that LH300 had the largest, whilst the LH210 fines had the smallest impact on the powder flow properties across the concentration range investigated.

As fluidization is a key step in delivering medication from a DPI formulation, characterization of the flow properties of the pre-blends under different states of aeration was also undertaken. The normalized fluidization energy (FE_{Norm}) measurements of the carrier blends are summarized in Table III. The increasing addition of LH230 had the largest impact on the FE_{Norm}, with 20 wt-% addition resulting in a value of 1.93 mJ/g compared to 0.70 mJ/g for LH100. The addition of LH300 increased the FE_{Norm} gradually with increasing levels of fines,

with a value of 1.75 mJ/g for the 20 wt-% pre-blend. The addition of LH210 had very little impact on FE_{Norm} at concentrations ≤ 10 wt-%. The addition of 20 wt-% was required for a more pronounced effect on the FE_{Norm} to a value of 1.60 mJ/g.

In summary, all the different parameters describing powder flow and fluidization characteristics suggest that the addition of the lactose fines into coarse lactose fractions does increase the cohesive properties of the carrier pre-blends.

Validation of BFE_{Norm} and FRI as measures of powder cohesion

The flow function (ff_c), BFE_{Norm} and FRI are all measures of powder cohesion, which is an important powder property for formulation processing. Measuring the powder flow properties using a shear cell tester (ff_c) is an established and widely accepted technique as the principles can be theoretically explained by Mohr circles (16,27). The dynamic approach used for example by the Freeman Technology FT4 powder rheometer (BFE_{Norm} and FRI) on the other hand is empirical and relies on characterizing differences amongst a group of powders based on their resistance to flow under a bulldozing action of an impeller blade, and relating the measurement results to the observed powder bulk behaviour during processing (17). Some theoretical work has been carried out to gain greater understanding of the powder properties affecting the results obtained on the dynamic FT4 system (30), but to date, the authors are not aware of experimental studies where the results obtained with the two different techniques have been compared. Therefore, to compare the results obtained by the two different techniques, and to validate the rheometry results obtained on the FT4 in this study, measurements of the lactose pre-blends were performed alongside Schulze RST-XS ring shear testing.

The ff_c values measured on the RST-XS system and BFE_{Norm} measured on the FT4 for the different lactose pre-blends are plotted against each other in Fig. 2. There is a correlation between ff_c and BFE_{Norm} over a range of lactose pre-blends containing either micronized or milled fines. The correlation suggests that for the lactose samples studied, the BFE_{Norm} measurements on the FT4 are comparable to the ff_c, and can be applied as a descriptor for the general powder flow properties for lactose blends containing either micronized or milled fines. However, while a correlation has been observed here for the series of lactose pre-blends, it has been suggested that such a correlation may not exist if a series of chemically different materials are characterized with static and dynamic measurement methods (15,17).

The FRI of the lactose carriers investigated in the current study are plotted against the flowability number ff_c in Fig. 3. The plot demonstrates a correlation between the FRI and ff_c,

and indicates that for free-flowing lactose carriers (ff_c > 4), the FRI was insensitive in distinguishing between powders with different cohesive properties. However, once ff_c was less than 3, the flow rate index became sensitive to the changes in the powder flow properties. These data suggest therefore that the FRI is relatively insensitive to Geldart type A powders, while being sensitive to the addition of Geldart type C powders at concentrations sufficient to affect its cohesive properties. This finding can be explained by the fact that FRI is known to be sensitive to the packing structure, and more precisely the air content, of the powder (17). Particles in free flowing powders pack closely and consequentially have low air content, and therefore altering the flow rate does not alter the contact between adjacent particles. In cohesive powders, on the other hand, air pockets remain within the powder packing structure. At slower flow rates the air has more time to escape, and thus the force transmission zone ahead of the blade extends upon slowing the flow rate, As a consequence the flow energy and FRI are increased (17).

The results presented in this section indicate that both the ff_c and BFE_{Norm} can be used for characterizing the general flow properties of lactose carriers used in DPI formulations. The results also suggest that in case of cohesive powders, FRI may provide additional insight into the general flow behaviour of the carrier pre-blends.

Mechanism by which the fine particle lactose regulates powder flow and fluidization properties

To investigate the link between the fine particle content of the carrier blends and their flow and fluidization properties, and to understand how the micronized and milled lactose fines increase the cohesion of the bulk powder, the ff_c values of the lactose carriers are plotted against the proportion of particles finer than 4.5 µm present in the pre-blends in Figure 4A. The figure demonstrates that the ff_c values for micronized fines (LH300) follow a very different trend to both the milled fines grades (LH230 and LH210). However, if the ff_c is plotted against the proportion of particles below 30 µm as per Figure 4B, the ff_c follows a single gradient when plotted against the amount of fines, independent of the type of fines added. This suggests that the size distribution of the particles <30 µm is less important than their overall proportion in determining flow properties. These findings are in agreement with a study by Guenette *et al.*, where it was shown that the fines below 10 µm had the largest negative effect on the flow properties of lactose carriers for inhalation, but that also the fines fraction between 10 and 40 µm decreased the powder flowability (25). In their study, it was shown that particles larger than 40 µm had no impact on the powder flow properties.

A plot of the normalized fluidization energy (FE_{Norm}) of the lactose pre-blends as a function of the percentage of particles <4.5 µm is shown in Figure 5A. These data suggest that the presence of micronized (LH300) fines had a different impact on the fluidization properties of the pre-blends than the milled fines (LH230 and LH210). For example, the addition of 10 wt-% LH300 resulted in a FE_{Norm} of approximately 1.2 mJ/g, whereas a similar proportion of milled fines (LH230 and LH210) produced a FE_{Norm} of approximately 1.6 mJ/g. The relationship between FE_{Norm} and the proportion of fines below 30 µm present in the carriers is illustrated in Figure 5B. These data are scattered to a greater extent than those shown in Figure 4B. This indicates that flow and fluidization characteristics of the lactose pre-blends may be governed by different mechanisms. Therefore, measuring the fluidization properties of the pre-blends in addition to the flow properties may add value to the characterization of lactose carriers for DPI formulations.

The flow and fluidization properties of the carriers indicate that addition of lactose fines to the carrier pre-blends increases the cohesion of the powder bulk both in terms of flow and fluidization properties. The data suggest that the increase in the cohesive strength is governed by the presence of lactose fines below approximately 30 µm, in agreement with the Geldart powder classification system (4).

In vitro performance of DPI formulations prepared with the lactose pre-blends as carriers

The *in vitro* aerosolization performance of budesonide formulations prepared using the lactose blends (Dose variation < 6% for all the blends) were tested with the Rotahaler and the Handihaler DPI devices, and are summarized in Table IV in terms of their fine particle fraction of emitted dose (FPF_{ED}) and mean mass aerodynamic diameter (MMAD) values. Rotahaler and Handihaler were chosen as the devices to represent opposite ends of the spectrum of capsule based devices such that a possible link between the powder properties and the aerosolization performance in different types of capsule based devices could be assessed.

Table IV highlights that only low concentrations of micronized fines are required to significantly improve DPI performance; in terms of fine particle fraction of emitted dose (FPF_{ED}), an addition of 5 wt-% or more of LH300 significantly ($p<0.01$) increased DPI formulation performance compared to the formulation prepared with LH100 alone on both the devices. These data suggest that the addition of micronized fines significantly affected the fine particle delivery performance of micronized budesonide in capsule based DPI devices. In the case of LH230, a 20 wt-% addition of the material was required to

significantly improve aerosolization performance compared to LH100 on both the devices. Across the range of concentrations investigated, the addition of LH210 did not significantly increase performance compared to LH100 ($p>0.05$). These data show that the addition of milled lactose fines to a carrier-based lactose formulation that is aerosolized from a capsule-based device does not necessarily improve DPI formulation performance. These findings are in agreement with previous studies by Zeng *et al.* and Adi *et al.* (11,24) that reported that micronized lactose fines were more efficient in improving DPI performance than coarser sized lactose fines.

To evaluate the extent of drug deagglomeration from the two different devices upon aerosolization, the mean mass aerodynamic diameters (MMAD) of budesonide aerosolized from the different formulations were inspected (Table IV). The MMAD of formulations containing LH300 remained unchanged over the range of fines concentrations for both the devices, suggesting that the extent of deagglomeration had not significantly changed for the formulations containing micronized fines despite the increasing fines content (Table IV). On the contrary, for the formulations prepared with the milled fines, LH230 and LH210, an increasing trend in the MMAD was measured as the fines content of the formulations was increased. For the Rotahaler, the MMAD was significantly higher for 5 and 10 wt-% LH230 formulations and the 10 and 20 wt-% LH210 formulations than for the LH100 formulation. For the Handihaler, formulations containing LH230 or LH210 had larger MMAD in comparison to the formulation prepared with LH100 only.

Due to the similar trends apparent in the results, the FPF_{ED} and MMAD data suggest that the drug deagglomeration from the two very different devices investigated here is governed by the powder properties rather than the device properties. Based on the data, it appears that micronized fines lead to a more complete and consistent deagglomeration behaviour over a range of fines concentrations, whereas with the milled fines less pronounced impact on drug delivery, but a more pronounced effect on MMAD of the drug is observed. These findings are in an agreement with a previous study, where changes in the values of MMAD were reported as lactose fines were added to DPI formulations. These changes were attributed the formation of drug-fines agglomerates that were distributed within the impactor (31).

However, although at first sight it appears that the device properties do not significantly alter the trends in DPI formulation performance at least in terms of FPF_{ED} and MMAD, on closer inspection differences between the two devices are observed in the proportion of emitted drug. This is illustrated in Figure 6, where the proportions of budesonide recovered from the device and capsule (Retained dose), and from the mouthpiece, throat, pre-separator and the

impactor stages (Emitted dose) on the two different devices from the different formulations are shown. The addition of micronized fines (LH300) increases the retained dose of budesonide for Rotahaler from approximately 30 to 45% over the range of the fines concentrations investigated (Figure 6A), whereas does not have an impact on the proportion of drug recovered from Handihaler, with the retained dose remaining constant at approximately 20% (Figure 6D). With finer of the milled fines, LH230, the retained dose of budesonide remains constant at ~30% until a fines concentration of 20 wt-%, when an increase to ~40% is observed (Figure 6B). With Handihaler, the retained dose remains constant at approximately 20% over the range of LH230 concentrations (Figure 6E). With the larger of the milled fines, LH210, the retained dose slightly increases from ~30 to 35% for Rotahaler over the range of concentrations (Figure 6C). With Handihaler, once again, no clear increasing trends are observed in the retention pattern over the range of fines concentrations (Figure 6F). These data suggest that Handihaler is capable of emptying the device and capsule in a consistent manner independent of the powder properties, whereas the device emptying efficiency of the Rotahaler may be dependent on the powder properties.

Therefore, *in vitro* performance data suggest that the powder properties govern the drug deagglomeration performance regardless of the device, whereas the device properties influence the efficiency of drug emission from the device and capsule during the aerosolization process. Therefore, to optimize drug delivery from a DPI product, it is recommended the powder properties are considered carefully when a low resistance device without a significant mechanism to aid capsule and device emptying is paired with a DPI formulation.

Relationship between powder flow and fluidization of the carrier-based lactose formulation and *in vitro* aerosolization performance

Fluidisation of the powder formulation is a key step in the aerosolisation process of APIs from DPI drug products. Furthermore, as the largest constituent of DPI formulations is the carrier lactose, then the fluidisation properties of the carrier lactose pre-blends may provide information regarding the aerosolization efficiency of DPI formulations. Indeed, recent studies have reported a correlation between carrier lactose fluidisation energy and *in vitro* performance of DPI model formulations (12,20), although opposing findings have also been reported especially in the case of ternary DPI formulations, where it was concluded that the measurements under aeration did not provide predictive capabilities for understanding DPI formulation performance (32). However, to further understand the possible mechanistic relationship between the fluidization properties of the carriers and the respective formulation

performance, the *in vitro* aerosolisation performance of the formulations was compared to the fluidization behaviour of the carriers.

The FPF_{ED} of the formulations used in the current study are plotted against the normalized fluidization energy (FE_{Norm}) of the carrier blend for each of the formulations and shown in Fig 7. In the case of the addition of micronized fines (LH300), there was a linear relationship between the energy required to fluidize the formulation and the fine particle fraction delivered up to 10 wt-% fines concentration with both the Rotahaler and the Handihaler (Figure 7A and 7C). However, at 20 wt-% concentration, despite the increase in the fluidization energy, the fine particle fraction decreased. Similarly, there was a linear relationship between fluidisation energy and FPF_{ED} for both the Rotahaler and Handihaler upon the addition of milled fines LH230 and LH210 (Figure 7B and 7D). However, as shown in Fig. 7, an increase in fluidization energy upon addition of milled fines only corresponded to a very slight improvement in the performance.

The current study has shown that on comparing the fluidization energy of a range of different lactose systems containing milled or micronized lactose fines, a universal correlation between the fluidisation energy and DPI performance is not strong. However, when comparing the fluidization energy and *in vitro* performance within a given lactose system, the relationship between fluidization energy and *in vitro* performance was established. These data therefore, suggest the fluidization energy measurement is more suitable for discriminating flow and fluidization properties between lactose systems that contain lactose fines of similar particle size. Therefore we suggest that powder flow and fluidisation measurements could potentially be used in routine manufacturing as an additional quality-by-design (QbD) tool for ensuring that the flow and fluidization characteristics of the raw material do not differ from what is normally used for a formulation. The findings of the current study also indicate that the increased cohesion theory (12) does not provide a universal explanation for improved DPI performance in the presence of lactose fines.

Conclusions

The current study showed that the addition of lactose fines increased the cohesion of the bulk powder and increased the fluidization energy of the lactose system. The increased cohesion of lactose pre-blends could be determined using both static and dynamic powder rheology measurements such as ff_c and BFE_{Norm}, respectively. It was shown that for characterising general powder flow properties, similar results are obtained with both the static and dynamic testing methods. Therefore, both these approaches can be

recommended for characterising general powder flow properties of lactose carriers used in DPI formulations. It was shown that amount of fines below 30 µm governed the powder flow and fluidisation properties of the lactose carriers and that the powder properties govern the deagglomeration properties of a formulation, whereas the device properties play a role in determining the extent of emitted dose. Increase in formulation performance was observed with micronized fines over the range of concentrations studied, whereas the addition of milled fines did not necessarily result in an improved formulation performance. There was no universal correlation observed between the fluidization properties and DPI performance, with milled and micronized fines producing different responses. The results therefore suggest that increased cohesion theory (12) does not universally explain the improved DPI performance in the presence of lactose fines. However, flow and fluidisation properties may be suited for predicting performance of formulations prepared with carriers of similar particle size characteristics and their use as an additional QbD tool in formulation manufacture can be recommended.

Acknowledgements

For DFE Pharma for funding the research and for Paul Vanden Branden of Scientific and Medical Products Ltd for access to a Schulze RST-XS ring shear tester.

References

1. Islam N, Gladki E. Dry powder inhalers (DPIs)--a review of device reliability and innovation. Int J Pharm. 2008;360:1–11.

2. Telko MJ, Hickey AJ. Dry powder inhaler formulation. Respir Care. 2005;50:1209–27.

3. Heyder J. Deposition of inhaled particles in the human respiratory tract and consequences for regional targeting in respiratory drug delivery. Proc Am Thorac Soc. 2004;1:315–20.

4. Geldart D. Types of gas fluidization. Powder Technology. 1973;7:285–92.

5. Visser J. Van der Waals and other cohesive forces affecting powder fluidization. Powder Technology. 1989;58:1–10.

6. Lucas P, Anderson K, Staniforth JN. Protein deposition from dry powder inhalers: fine particle multiplets as performance modifiers. Pharm. Res. 1998;15:562–9.

7. Jones MD, Hooton JC, Dawson ML, Ferrie AR, Price R. An investigation into the dispersion mechanisms of ternary dry powder inhaler formulations by the quantification of interparticulate forces. Pharm. Res. 2008;25:337–48.

8. Ganderton D. The generation of respirable clouds from coarse powder aggregates. J Biopharm Sci. 1992;3:101–5.

9. Young PA, Edge S, Traini D, Jones MD, Price R, El-Sabawi D, et al. The influence of dose on the performance of dry powder inhalation systems. Int J Pharm. 2005;296:26–33.

10. Hersey JA. Ordered mixing: a new concept in powder mixing practice. Powder Technology. 1975;11:41–4.

11. Zeng XM, Martin GP, Tee SK, Ghoush AA, Marriott C. Effects of particle size and adding sequence of fine lactose on the deposition of salbutamol sulphate from a dry powder formulation. Int J Pharm. 1999;182:133–44.

12. Shur J, Harris H, Jones MD, Kaerger JS, Price R. The role of fines in the modification of the fluidization and dispersion mechanism within dry powder inhaler formulations. Pharm. Res. 2008;25:1631–40.

13. Veersteeg H, Hargreave G, Hind R. An optical study of aerosol generation in dry powder inhalers. Drug Delivery to the Lungs 16. Edinburgh; 2005. pp. 3–6.

14. Tuley R, Shrimpton J, Jones MD, Price R, Palmer M, Prime D. Experimental observations of dry powder inhaler dose fluidisation. Int J Pharm. 2008;358:238–47.

15. Krantz M, Zhang H, Zhu J. Characterization of powder flow: Static and dynamic testing. Powder Technology. 2009**;**194:239-45.

16. Schulze D. Flow properties of powders and bulk solids. Braunschweig/Wolfenbu ttel. 2006. http://www.dietmar-schulze.com/grdle1.pdf Accessed on 25/01/2014

17. Freeman R. Measuring the flow properties of consolidated, conditioned and aerated powders—a comparative study using a powder rheometer and a rotational shear cell. Powder Technology 2007;174:25–33.

18. Zhou Q, Armstrong B, Larson I, Stewart PJ, Morton DAV. Improving powder flow properties of a cohesive lactose monohydrate powder by intensive mechanical dry coating. J Pharm Sci. 2010;99:969–81.

19. Zhou QT, Denman JA, Gengenbach T, Das S, Qu L, Zhang H, et al. Characterization of the surface properties of a model pharmaceutical fine powder modified with a pharmaceutical lubricant to improve flow via a mechanical dry coating approach. J Pharm Sci. 2011;100:3421–30.

20. Pitchayajittipong C, Price R, Shur J, Kaerger JS, Edge S. Characterisation and functionality of inhalation anhydrous lactose. Int J Pharm. 2010;390:134–41.

21. Crowder T, Hickey A. Powder specific active dispersion for generation of pharmaceutical aerosols. Int J Pharm. 2006;327:65–72.

22. Le VNP, Robins E, Flament MP. Air permeability of powder: a potential tool for Dry Powder Inhaler formulation development. Eur J Pharm Biopharm. 2010;76:464–9.

23. Adi H, Larson I, Chiou H, Young P, Traini D, Stewart P. Agglomerate strength and dispersion of salmeterol xinafoate from powder mixtures for inhalation. Pharm. Res. 2006;23:2556–65.

24. Handoko A, Ian L, Peter SJ. Influence of the polydispersity of the added fine lactose on the dispersion of salmeterol xinafoate from mixtures for inhalation. Eur J Pharm Sci. 2009;36:265–74.

25. Guenette E, Barrett A, Kraus D, Brody R, Harding L, Magee G. Understanding the effect of lactose particle size on the properties of DPI formulations using experimental design. Int J Pharm. 2009;380:80–8.

26. Kubavat HA, Shur J, Ruecroft G, Hipkiss D, Price R. Influence of primary crystallisation conditions on the mechanical and interfacial properties of micronised budesonide for dry powder inhalation. Int J Pharm. 2012;430:26–33.

27. Schwedes J, Schulze D. Measurement of flow properties of bulk solids. Powder Technology. 1990;61:59–68.

28. Shur J, Lee S, Adams W, Lionberger R, Tibbatts J, Price R. Effect of device design on the in vitro performance and comparability for capsule-based dry powder inhalers. AAPS J. 2012;14:667–76.

29. Louey MD, Razia S, Stewart PJ. Influence of physico-chemical carrier properties on the in vitro aerosol deposition from interactive mixtures. Int J Pharm. 2003;252:87–98.

30. Bharadwaj R, Ketterhagen WR, Hancock BC. Discrete element simulation study of a Freeman powder rheometer. Chemical Engineering Science. 2010;65:5746–56.

31. Podczeck F. The influence of particle size distribution and surface roughness of carrier particles on the in vitro properties of dry powder inhalations. Aerosol Science and Technology. 1999**;**31:301–21.

32. Cordts E, Steckel H. Capabilities and limitations of using powder rheology and permeability to predict dry powder inhaler performance. Eur. J. Pharm. Biopharm. 2012;82(2):417-23.

Tables

Table I Particle size distributions of the coarse lactose (LH100) and the lactose fines (LH300, LH230 and LH210) used in the study in terms of d10, d50 and d90 of density distributions. The data represents mean ± standard deviation (S.D.), n=5.

	d10 ± S.D. (µm)	**d50 ± S.D. (µm)**	**d90 ± S.D. (µm)**
LH100	42.21 ± 0.46	101.59 ± 0.40	157.80 ± 0.51
LH300	0.84 ± 0.01	2.41 ± 0.07	7.76 ± 0.27
LH230	1.31 ± 0.01	8.05 ± 0.06	21.97 ± 0.09
LH210	1.64 ± 0.01	14.3 ± 0.22	39.45 ± 0.54

Table II Particle size distributions of the lactose carriers used in the study in terms of d10, d50 and d90. The data represents mean ± standard deviation (S.D.), n=5. In addition, the mean values (n=5) of proportion of particles finer than 4.5 and 30 µm present in the carriers are tabulated.

	d10 ± S.D. (µm)	**d50 ± S.D. (µm)**	**d90 ± S.D. (µm)**	**<4.5 µm (%)**	**<30 µm (%)**
LH100	44.30 ± 1.58	103.37 ± 1.01	159.62 ± 0.56	1.29	6.24
+2.5% LH300	23.44 ± 1.01	99.66 ± 0.35	161.02 ± 2.15	4.88	11.48
+5% LH300	5.22 ± 0.32	95.19 ± 0.79	157.27 ± 3.31	9.34	17.03
+10% LH300	2.08 ± 0.02	87.30 ± 0.85	154.55 ± 3.77	17.43	26.97
+20% LH300	1.73 ± 0.06	60.76 ± 2.11	139.93 ± 3.40	23.04	42.75
+2.5% LH230	26.41 ± 0.84	99.78 ± 0.37	160.88 ± 0.31	2.76	10.95
+5% LH230	14.70 ± 0.29	96.58 ± 0.64	159.82 ± 3.02	4.32	15.13
+10% LH230	7.33 ± 0.14	89.55 ± 0.38	156.65 ± 1.02	7.23	23.23
+20% LH230	3.26 ± 0.21	67.18 ± 1.55	134.32 ± 2.77	12.47	38.15
+2.5% LH210	31.53 ± 1.05	100.23 ± 0.64	158.57 ± 2.12	1.98	9.56
+5% LH210	23.63 ± 0.61	97.72 ± 0.62	159.85 ± 1.74	2.62	12.27
+10% LH210	14.25 ± 0.27	91.51 ± 0.70	156.18 ± 3.04	4.08	17.89
+20% LH210	8.72 ± 0.12	79.30 ± 1.53	151.45 ± 6.27	6.02	26.79

Table III Summary of the powder flow and fluidization properties of the carriers as characterized by flowability number (ff_c), normalized basic flow energy (BFE_{Norm}), flow rate index (FRI), Normalized fluidization energy (FE_{Norm}), dynamic flow index (DFI), Carr's index and Hausner ratio. The data represents mean ± Standard deviation (S.D.), n=3.

	ff_c ± S.D.	**BFE_{Norm} ± S.D. (mJg^{-1})**	**FRI ± S.D.**	**FE_{Norm} ± S.D. (mJg^{-1})**
LH100	5.55±0.23	25.12±0.40	1.02±0.01	0.70±0.08
+2.5% LH300	4.35±0.25	22.06±0.31	1.10±0.01	0.84±0.09
+5% LH300	3.43±0.10	20.34±0.49	1.19±0.02	1.23±0.07
+10% LH300	2.25±0.06	15.68±0.54	1.52±0.02	1.44±0.07
+20% LH300	1.63±0.02	9.93±0.14	2.41±0.15	1.75±0.01
+2.5% LH230	4.28±0.26	21.65±0.11	1.06±0.00	0.95±0.10
+5% LH230	3.45±0.37	19.37±0.17	1.09±0.00	1.12±0.13
+10% LH230	2.59±0.04	16.07±0.15	1.29±0.01	1.54±0.10
+20% LH230	1.74±0.03	10.52±0.33	1.81±0.06	1.93±0.17
+2.5% LH210	4.97±0.13	23.48±0.42	1.03±0.01	0.78±0.02
+5% LH210	4.14±0.19	21.11±0.59	1.06±0.05	1.00±0.14
+10% LH210	3.51±0.14	19.54±0.31	1.14±0.01	1.04±0.09
+20% LH210	2.28±0.02	13.24±0.10	1.41±0.02	1.60±0.03

Table IV *In vitro* performance of the formulations prepared with the lactose pre-blends as the carriers in terms of fine particle fraction of emitted dose (FPF_{ED}) and mean mass aerodynamic diameter (MMAD). The data for FPF_{ED} represents mean ± standard deviation, n=3. The data for MMAD represents mean ± geometric standard deviation (GSD), n=3.

	Rotahaler		**Handihaler**	
	FPF_{ED} ± S.D. (%)	**MMAD ± GSD (µm)**	**FPF_{ED} ± S.D. (%)**	**MMAD ± GSD (µm)**
LH100	15.68 ± 0.42	3.28 ± 1.92	15.21 ± 1.55	3.00 ± 1.81
+2.5% LH300	20.18 ± 1.56	3.73 ± 1.79	22.72 ± 2.42	3.16 ± 1.74
+5% LH300	28.37 ± 2.26	3.71 ± 1.77	33.94 ± 1.78	3.01 ± 1.73
+10% LH300	40.02 ± 4.03	3.41 ± 1.82	43.07 ± 0.62	2.95 ± 1.77
+20% LH300	37.80 ± 3.43	3.48 ± 1.96	37.00 ± 4.39	3.22 ± 1.87
+2.5% LH230	17.31 ± 3.02	3.50 ± 2.02	17.63 ± 1.11	3.26 ± 1.90
+5% LH230	16.13 ± 1.95	4.31 ± 1.86	20.84 ± 3.39	3.31 ± 1.97
+10% LH230	20.92 ± 2.55	4.40 ± 1.87	22.50 ± 2.10	3.62 ± 1.98
+20% LH230	32.07 ± 2.85	3.74 ± 2.12	31.51 ± 0.31	3.45 ± 2.08
+2.5% LH210	14.52 ± 1.34	3.60 ± 1.88	16.18 ± 0.70	3.26 ± 1.80
+5% LH210	15.39 ± 2.57	3.66 ± 1.89	18.27 ± 0.21	3.34 ± 1.87
+10% LH210	18.11 ± 3.33	4.13 ± 1.83	19.36 ± 3.67	3.41 ± 1.85
+20% LH210	17.95 ± 0.94	4.04 ± 2.05	18.82 ± 1.08	3.56 ± 2.04

Legend to Figures

Figure 1 900x magnification scanning electron micrographs of A) LH100 B) LH300 C) LH230 and D) LH210

Figure 2 The relationship between the ff_c number measured on the Schulze RST-XS ring shear tester and the normalized basic flow energy (BFE_{Norm}) measured on the FT4 powder rheometer for the individual lactose pre-blends investigated in the study. The data represents mean ± standard deviation, n=3.

Figure 3 The relationship between flow rate index (FRI) and flowability number ff_c for the lactose carriers investigated in the study. The data represents mean ± standard deviation, n=3.

Figure 4 The relationship between ff_c and the proportion of fines A) <4.5µm and B) <30µm in the different lactose pre-blends. The data for ff_c represents mean ± standard deviation, n=3. The data for proportion of particles finer than 4.5 µm and 30 µm represents mean of 5 determinations.

Figure 5 The relationship between the proportion of fines below A) 4.5 µm and B) 30 µm present in the carrier and the normalized fluidization energy (FE_{Norm}) of the lactose pre-blends. The data for FE_{Norm} represents mean ± standard deviation, n=3. The data for proportion of particles finer than 4.5 µm and 30 µm represents mean of 5 determinations.

Figure 6 The proportion of budesonide recovered the device and capsule (Retained dose, black bars) and from mouthpiece, throat, pre-separator and impactor stages (Emitted dose, grey bars) for the series of formulations prepared with A) LH300, B) LH230 and C) LH210 aerosolized on a Rotahaler and D) LH300, E) LH230 and F) LH210 aerosolized on a Handihaler. The data represents the mean of three repeated determinations.

Figure 7 The relationship between the normalized fluidization energy (FE_{Norm}) of the carrier pre-blends and the DPI performance in terms of fine particle fraction of emitted dose (FPF_{ED}) for formulations prepared with A) micronized (LH300) and B) milled fines (LH230 and LH210) aerosolized on a Rotahaler and C) micronized (LH300) and D) milled fines (LH230 and LH210) aerosolized on a Handihaler. The data represents mean ± standard deviation, n=3.

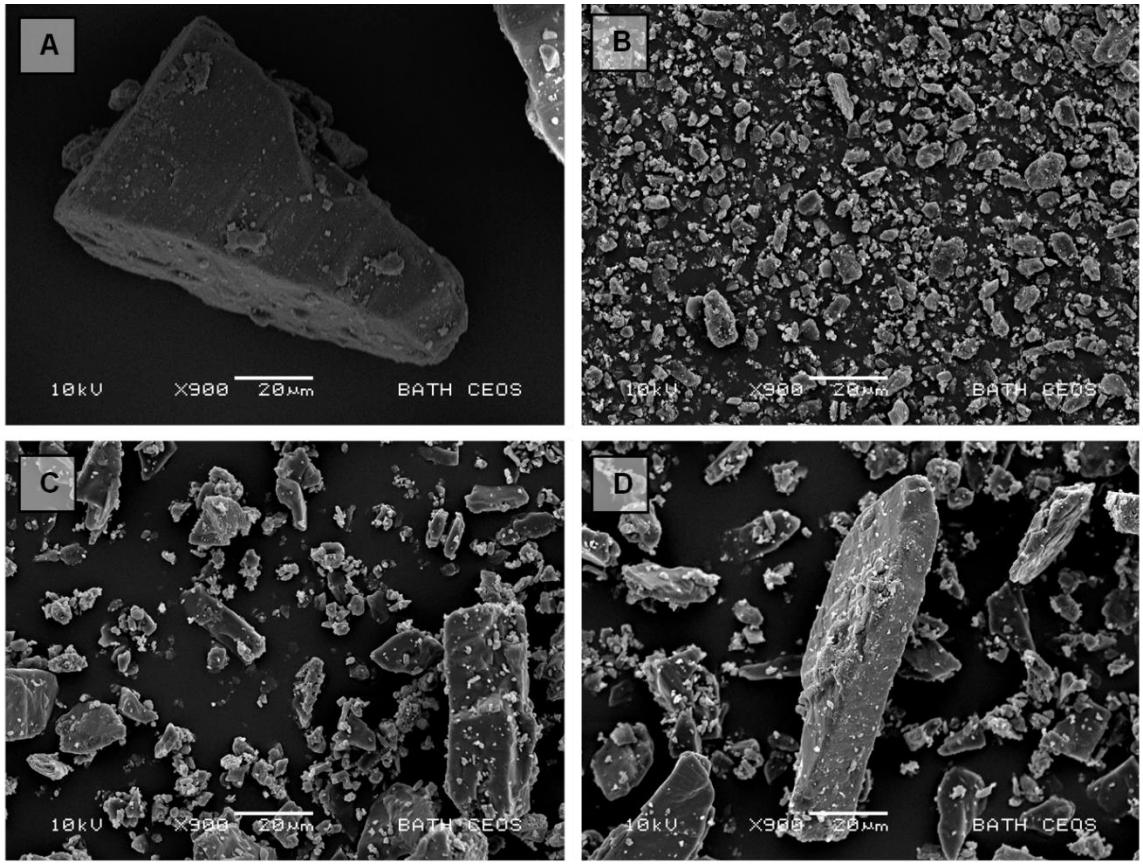
A
10kV X900 20µm BATH CEOS
B
10kV X900 20µm BATH CEOS
C
10kV X900 20µm BATH CEOS
D
10kV X900 20µm BATH CEOS

Figure 1.

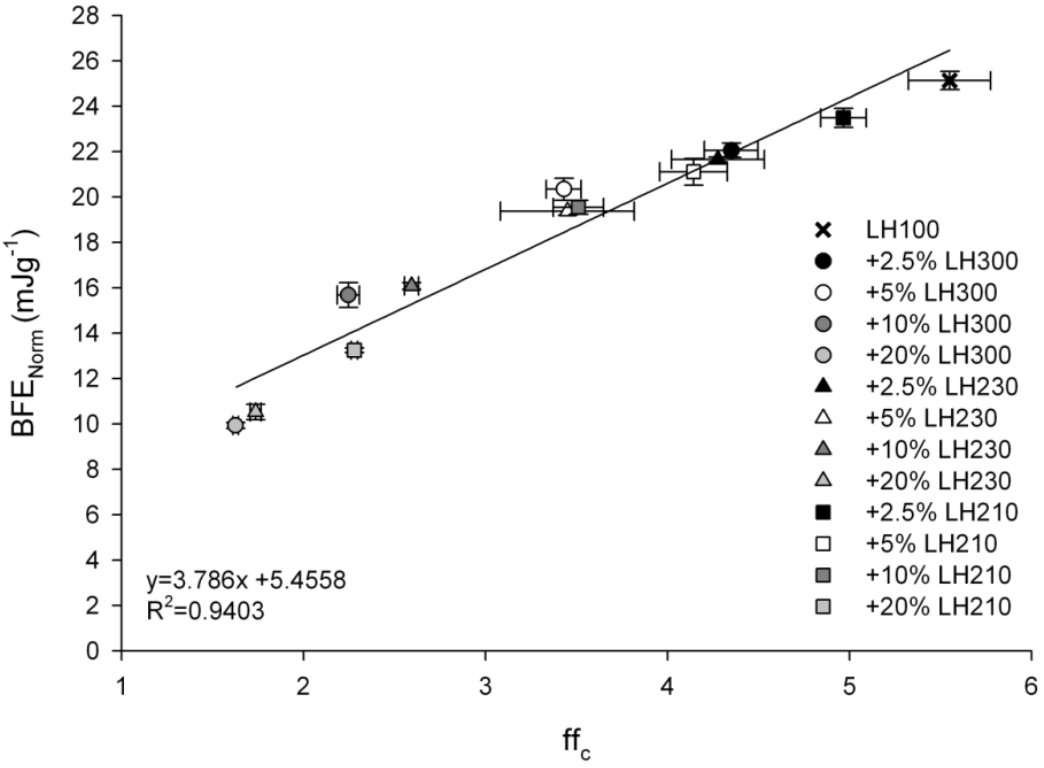
BFE$_{Norm}$ (mJg^{-1})
ff$_c$
y=3.786x +5.4558
R^2=0.9403
LH100
+2.5% LH300
+5% LH300
+10% LH300
+20% LH300
+2.5% LH230
+5% LH230
+10% LH230
+20% LH230
+2.5% LH210
+5% LH210
+10% LH210
+20% LH210

Figure 2.

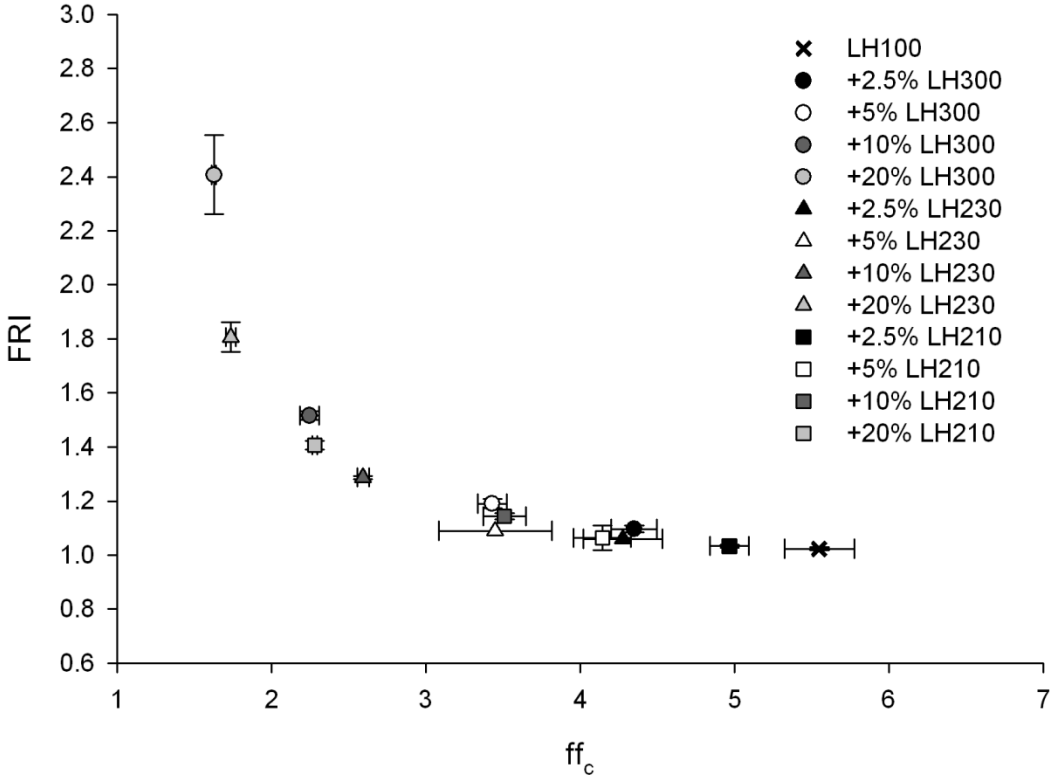
FRI
ff$_c$
3.0
2.8
2.6
2.4
2.2
2.0
1.8
1.6
1.4
1.2
1.0
0.8
0.6
1
2
3
4
5
6
7
LH100
+2.5% LH300
+5% LH300
+10% LH300
+20% LH300
+2.5% LH230
+5% LH230
+10% LH230
+20% LH230
+2.5% LH210
+5% LH210
+10% LH210
+20% LH210

Figure 3.

A)

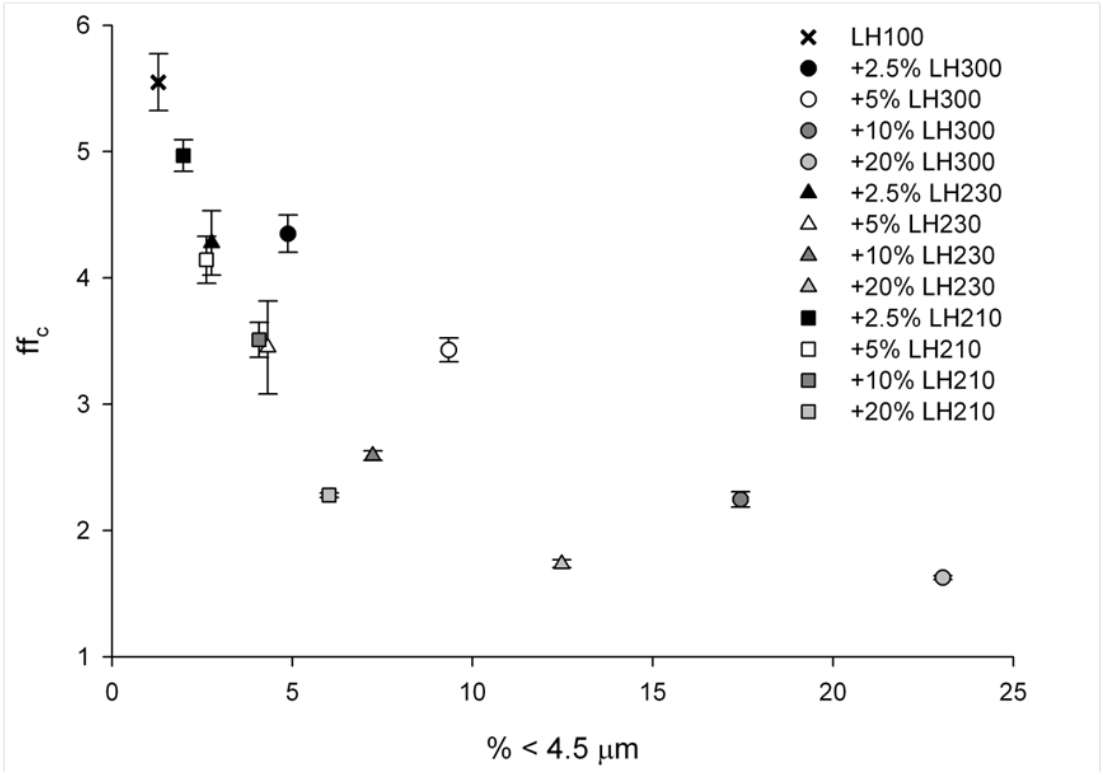
LH100
+2.5% LH300
+5% LH300
+10% LH300
+20% LH300
+2.5% LH230
+5% LH230
+10% LH230
+20% LH230
+2.5% LH210
+5% LH210
+10% LH210
+20% LH210
ffc
% < 4.5 μm

B)

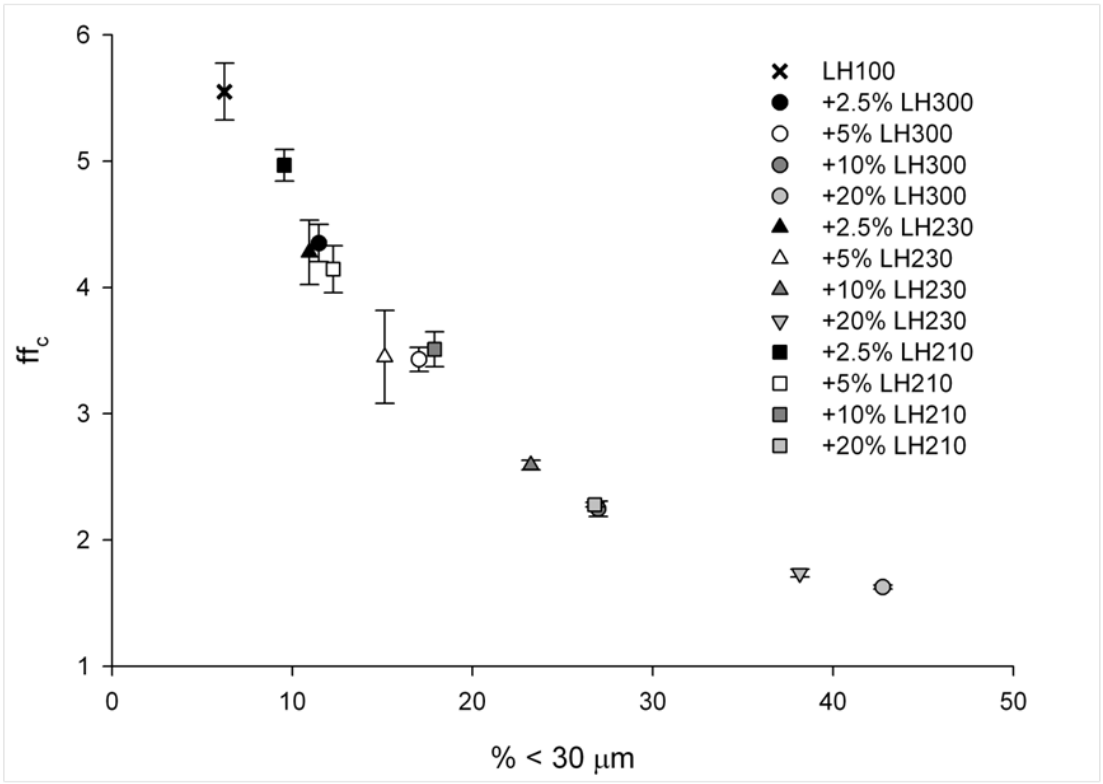
LH100
+2.5% LH300
+5% LH300
+10% LH300
+20% LH300
+2.5% LH230
+5% LH230
+10% LH230
+20% LH230
+2.5% LH210
+5% LH210
+10% LH210
+20% LH210
ffc
% < 30 μm

Figure 4.

A)

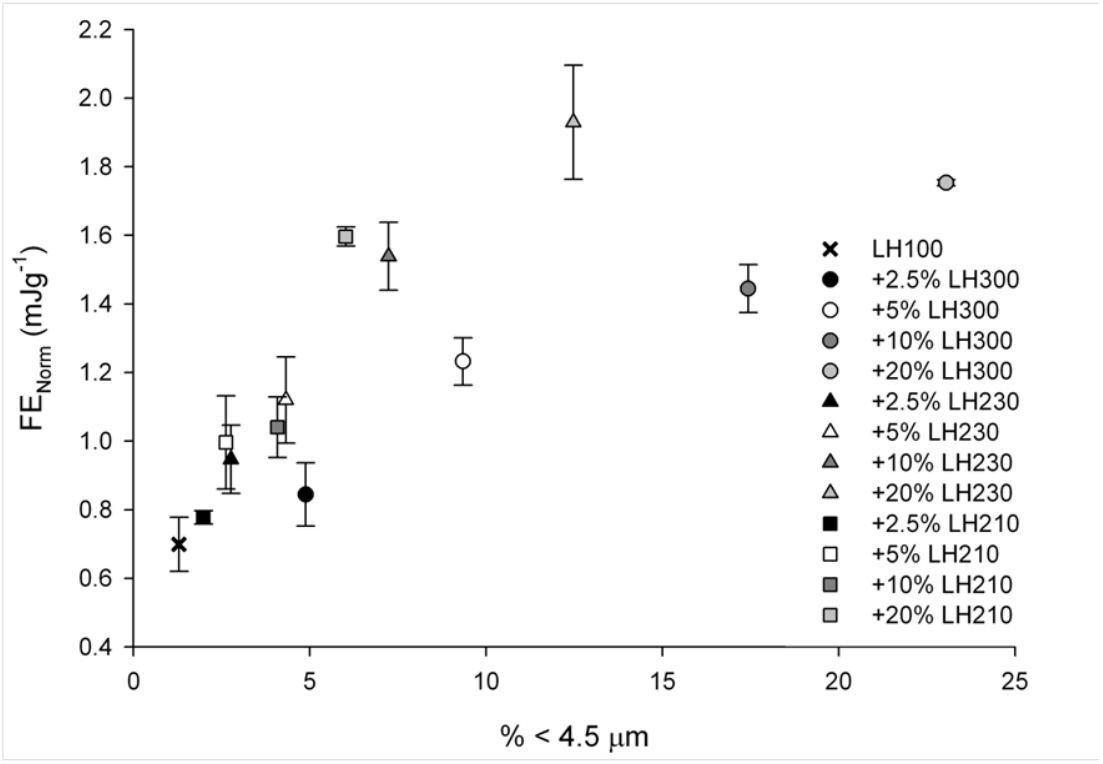
2.2
2.0
1.8
1.6
1.4
1.2
1.0
0.8
0.6
0.4
FE_Norm (mJg-1)
0
5
10
15
20
25
% < 4.5 μm
LH100
+2.5% LH300
+5% LH300
+10% LH300
+20% LH300
+2.5% LH230
+5% LH230
+10% LH230
+20% LH230
+2.5% LH210
+5% LH210
+10% LH210
+20% LH210

B)

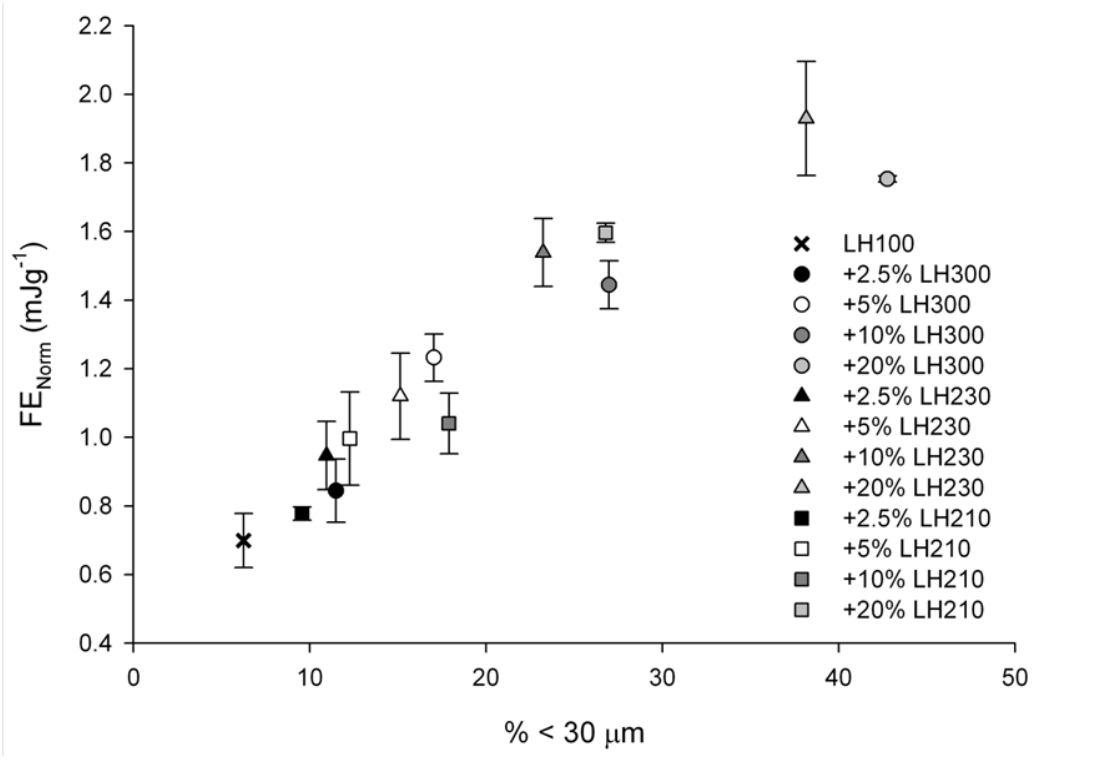
2.2
2.0
1.8
1.6
1.4
1.2
1.0
0.8
0.6
0.4
FE_Norm (mJg-1)
0
10
20
30
40
50
% < 30 μm
LH100
+2.5% LH300
+5% LH300
+10% LH300
+20% LH300
+2.5% LH230
+5% LH230
+10% LH230
+20% LH230
+2.5% LH210
+5% LH210
+10% LH210
+20% LH210

Figure 5.

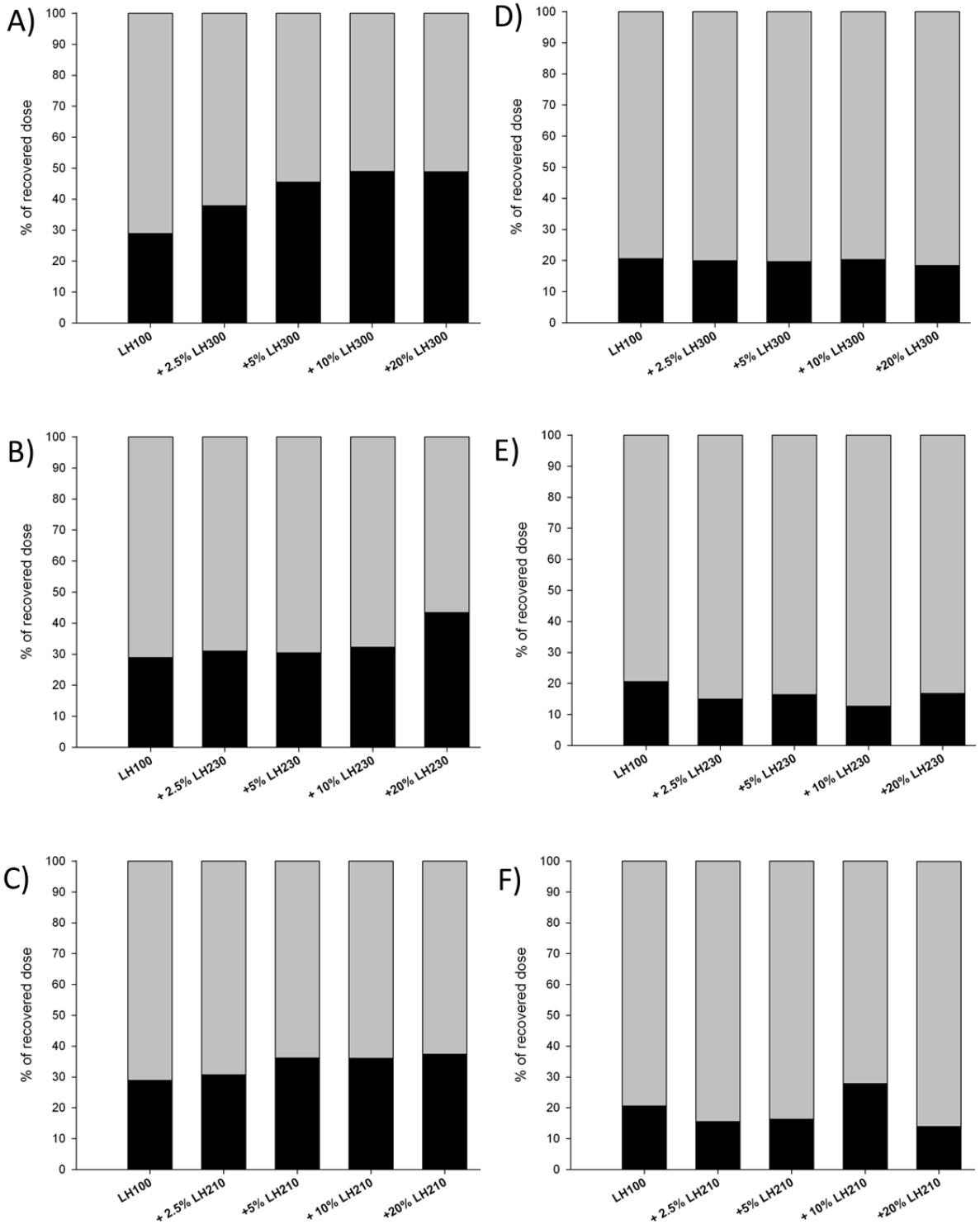
A)
% of recovered dose
LH100
+ 2.5% LH300
+5% LH300
+ 10% LH300
+20% LH300
D)
% of recovered dose
LH100
+ 2.5% LH300
+5% LH300
+ 10% LH300
+20% LH300
B)
% of recovered dose
LH100
+ 2.5% LH230
+5% LH230
+ 10% LH230
+20% LH230
E)
% of recovered dose
LH100
+ 2.5% LH230
+5% LH230
+ 10% LH230
+20% LH230
C)
% of recovered dose
LH100
+ 2.5% LH210
+5% LH210
+ 10% LH210
+20% LH210
F)
% of recovered dose
LH100
+ 2.5% LH210
+5% LH210
+ 10% LH210
+20% LH210

Figure 6.

A)

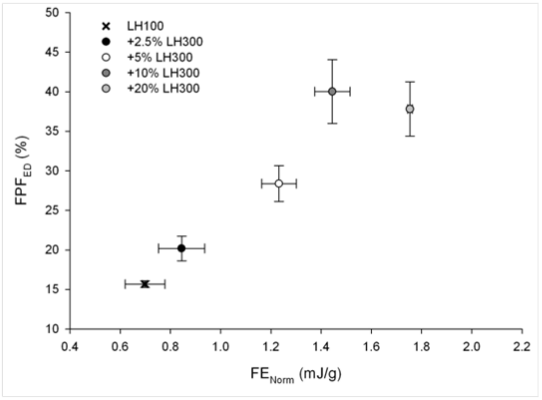

B)

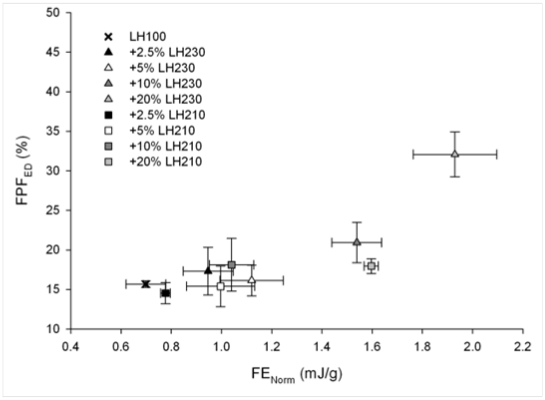

C)

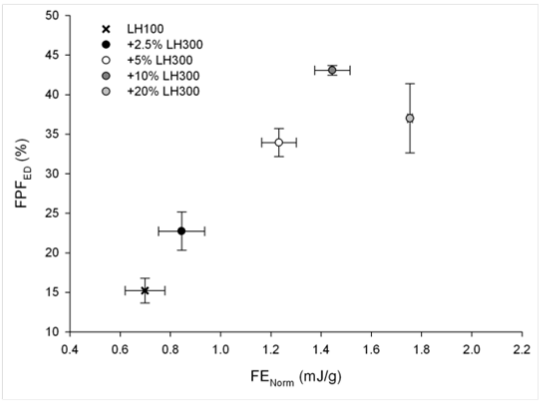

D)

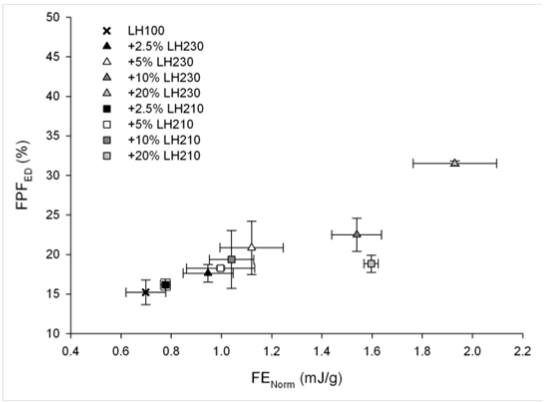

Figure 7.